Cell Death and Differentiation (2016) 23, 776–786

www.nature.com/cdd

OPEN

Tripartite containing motif 32 modulates proliferation of human neural precursor cells in HIV-1 neurodegeneration

M Fatima[1], R Kumari[1], JC Schwamborn[2], A Mahadevan[3], SK Shankar[3], R Raja[4] and P Seth*[,1]

In addition to glial cells, HIV-1 infection occurs in multipotent human neural precursor cells (hNPCs) and induces quiescence in NPCs. HIV-1 infection of the brain alters hNPC stemness, leading to perturbed endogenous neurorestoration of the CNS following brain damage by HIV-1, compounding the severity of dementia in adult neuroAIDS cases. In pediatric neuroAIDS cases, HIV-1 infection of neural stem cell can lead to delayed developmental milestones and impaired cognition. Using primary cultures of human fetal brain-derived hNPCs, we gained novel insights into the role of a neural stem cell determinant, tripartite containing motif 32 (TRIM32), in HIV-1 Tat-induced quiescence of NPCs. Acute HIV-1 Tat treatment of hNPCs resulted in proliferation arrest but did not induce differentiation. Cellular localization and levels of TRIM32 are critical regulators of stemness of NPCs. HIV-1 Tat exposure increased nuclear localization and levels of TRIM32 in hNPCs. The *in vitro* findings were validated by studying TRIM32 localization and levels in frontal cortex of HIV-1-seropositive adult patients collected at post mortem as well as by infection of hNPCs by HIV-1. We observed increased percentage of cells with nuclear localization of TRIM32 in the subventricular zone (SVZ) as compared with age-matched controls. Our quest for probing into the mechanisms revealed that TRIM32 is targeted by miR-155 as downregulation of miR-155 by HIV-1 Tat resulted in upregulation of TRIM32 levels. Furthermore, miR-155 or siRNA against TRIM32 rescued HIV-1 Tat-induced quiescence in NPCs. Our findings suggest a novel molecular cascade involving miR-155 and TRIM32 leading to HIV-1 Tat-induced attenuated proliferation of hNPCs. The study also uncovered an unidentified role for miR-155 in modulating human neural stem cell proliferation, helping in better understanding of hNPCs and diseased brain.
Cell Death and Differentiation (2016) **23,** 776–786; doi:10.1038/cdd.2015.138; published online 20 November 2015

Failure to eliminate HIV-1 from brain limits its eradication from AIDS patient. Despite success of antiretroviral therapies in reducing systemic viral load and severe dementia, milder forms of HIV-1-associated neurological disorder (HAND) still prevail because of poor penetrance of combinatorial antiretroviral therapy (cART) drugs into the brain.[1–4]

HIV-1 infects majority of brain cells, including neural precursor cells (NPCs).[5–8] Viral infection of NPCs impairs the ability of the brain for endogenous neurorestoration by differentiating existing NPCs, as viral proteins interfere with the self-renewing capability of the precursors cells and perturbing their commitment toward neuronal lineage[9,10] in adult neuroAIDS cases. The severity of the NPCs being affected by HIV-1 is also a major concern in pediatric ages, as HIV-1 infection can result in cognitive impairment as well as deranged brain development, brain atrophy and cerebrovascular abnormalities.[11] In addition to this, the NPCs are also considered as a reservoir for the latent virus.[6]

To gain insights into cellular cascades important for HIV-1 Tat-mediated quiescence of NPCs, we searched for cellular stemness determinants and their association with HIV-1. We identified tripartite containing motif 32 (TRIM32), a HIV-1 Tat interacting protein,[12] that also regulates stemness of NPCs.[13–15] Hence, we explored the possibility of association of these two properties of TRIM32.

TRIM32 is a member of TRIM family comprising 75 members,[16] many of which including TRIM32 are critical to innate immune response to viral replication.[16–21] TRIM32 has been implicated in limb girdle muscular dystrophy,[22] Bardet–Biedl syndrome,[23] epidermal carcinogenesis,[24] Alzheimer's disease[25]and stress-induced anxiety and depressive behavior.[26] By interacting with Argonaute, TRIM32 collaborates with the miRNA machinery activating particular microRNAs[13] and regulates retinoic acid-mediated neuronal differentiation.[27]

As HIV-1 Tat and TRIM32 influence stemness of NPCs and are interacting proteins, we investigated whether TRIM32 mediates the effects of HIV-1 Tat on stemness of NPCs.

Results

HIV-1 impairs stemness of neural progenitor cells. HIV-1 induces quiescence in human NPCs (hNPCs) as the HIV-1-infected brain autopsy tissue showed lower Ki67 (a proliferation marker)-positive cells in hippocampal sections

[1]Cellular and Molecular Neuroscience, National Brain Research Centre, Manesar (Gurgaon), Haryana, India; [2]Luxembourg Centre for Systems Biomedicine (LCSB), University of Luxembourg, 7, Avenue des Hauts-Fourneaux, L-4362, Campus Belval, Esch-sur-Alzette, Luxembourg; [3]Department of Neuropathology, National Institute of Mental Health & Neurosciences, Bangalore, India and [4]Laboratory of Virology, National Institute of Immunology, New Delhi, India
*Corresponding author: P Seth, Cellular and Molecular Neuroscience, National Brain Research Centre (NBRC), NH-8, Nainwal Road, Manesar, Haryana 122051, India. Tel: +91 124 2845212; Fax: +91 124 2338928; E-mail: pseth@nbrc.ac.in
Abbreviations: TRIM32, tripartite containing motif 32; hNPC, human neural precursor cell; SVZ, subventricular zone
Received 24.1.15; revised 14.8.15; accepted 11.9.15; Edited by M Piacentini; published online 20.11.15

as compared with the controls.[28] To analyze whether HIV-1 infection affected stemness of the NPCs, we examined nestin positivity in the subventricular zone (SVZ) in brain sections from the frontal cortex that included the angle of lateral ventricle. Periventricular brain sections of HIV-1-infected patients showed lower number of nestin-positive precursor cells as compared with age-matched controls. In control sections, nestin positivity was observed to be $12.9 \pm 4.9\%$ in the SVZ, whereas in HIV-1-infected brain sections, a significant decrement was observed in the percentage of nestin-positive cells ($3 \pm 2.0\%$; $P < 0.05$; Figure 1).

Nuclear translocation of TRIM32 in response to HIV-1 Tat. Cellular localization of TRIM32 is crucial in determining stemness of the neural stem cells. TRIM32 translocates to nucleus following neuronal differentiation signal where it ubiquitinates c-myc and arrests the proliferation so as to initiate neurogenesis.[14] To examine TRIM32 localization in precursor cells, autopsied control adult and fetal brain sections were probed for TRIM32. It was observed that TRIM32 was localized differentially in the SVZ. Microscopic examination revealed that most of the cells had TRIM32 localized to the cytoplasm, others had TRIM32 localized to both cytoplasmic and nuclear TRIM32 and rarely the cells had TRIM32 within the nucleus (Supplementary Figure S2A). These cells were confirmed to be neural stem cells by probing them for nestin in serial sections (Supplementary Figure S2B). In our culture system, TRIM32 was localized in both cytoplasm and nucleus in hNPCs.

As nuclear translocation of TRIM32 can arrest the proliferation in hNPCs, we investigated whether HIV-1 Tat affects the localization of TRIM32 by ICC following 24 h of exposure to HIV-1 Tat. Cells were analyzed under two groups: (1) consisted cells with TRIM32 in both nucleus and cytoplasm and (2) cells with exclusively nuclear localization of TRIM32. The percentage of cells showing cytoplasmic and nuclear localization of TRIM32 was 62.2% in control compared with 4.7% in Tat-treated test group ($P < 0.005$). Furthermore, when TRIM32 nuclear localization was assayed, we found that 37.8% of cells had TRIM32 in nucleus in control conditions, whereas in Tat-treated group this percentage increased to 95.3% ($P < 0.005$; Figure 2a).

The hNPCs were transfected with HIV-1 Tat expressing pDs Red vector so that Tat-transfected cells could be easily visualized with Ds Red tag. ICC was performed to assess localization of TRIM32. TRIM32 colocalized with HIV-1 Tat in the nucleus and cytoplasm. In cells where Tat had translocated completely into the nucleus, TRIM32 also localized entirely within the nucleus (Figure 2b), suggesting an association between the two.

Tat-induced nuclear localization of TRIM32 in hNPCs was further confirmed by western blotting in nuclear and cytosolic extracts from hNPCs treated with HIV-1 Tat for 24 h. Nuclear extracts showed an increase of 43% ($P < 0.005$) with concomitant decrease of 34.6% of TRIM32 in the cytosolic levels ($P < 0.0005$) as compared with the control (Figure 2c).

To validate our *in vitro* findings, we probed for TRIM32 in SVZ region in human brain sections from HIV-1-infected subjects and age-matched control brain sections. In controls, TRIM32 was entirely cytoplasmic in 70.5% of the cells, but in

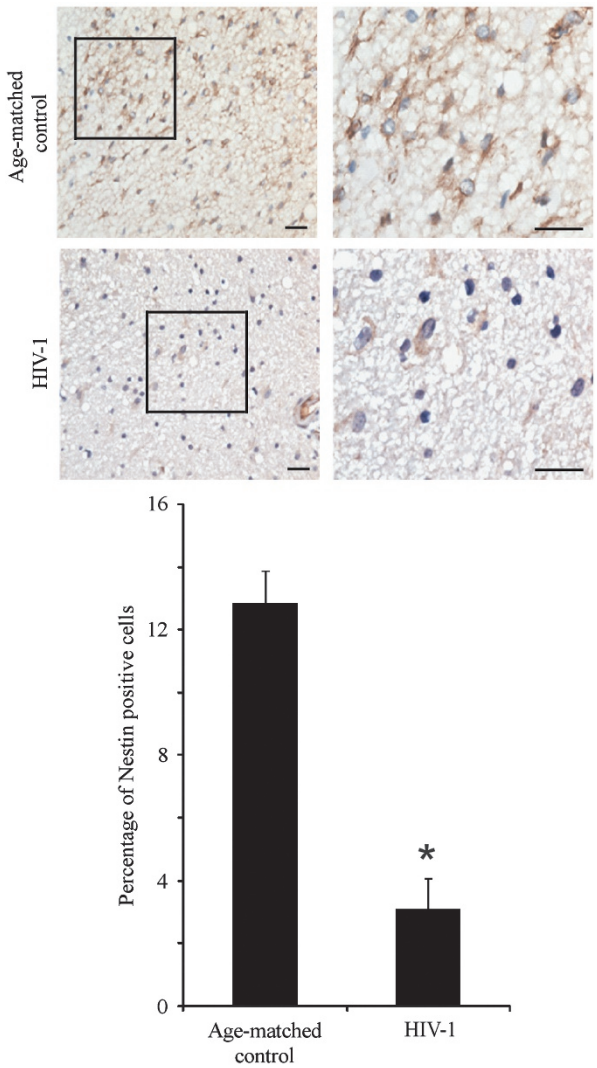

Figure 1 HIV-1 impairs stemness of neural progenitor cells. Immunohistochemical analysis of SVZ region for nestin-positive neural precursor cells in adult human brain for indicated groups. DAB stain (brown) shows nestin-positive cells. Right panel shows magnified images from the inset. Scale, 50 μm. Lower panel shows bar graph that represents percentage of Nestin-positive cells in the SVZ region of controls and HIV-1-infected individuals. The data are a representation of findings from four age-matched controls and HIV-1-infected brain sections (mean $\pm$ S.D.). *$P < 0.05$ as compared with control

HIV-1-infected brain sections this percentage was decreased to mere 5.0% ($P < 0.005$). In control sections, there were only 7.9% of cells with exclusive nuclear TRIM32, whereas in HIV-1-infected sections this percentage was a staggering 69.1% ($P < 0.05$; Figure 2d). To confirm that the nuclear translocation of TRIM32 was correlated with viral infection in the brain, we also performed viral detection through p24 staining in serial section from a similar area of the same patient and observed substantial staining for HIV-1 p24 antigen (Supplementary Figure S3). These *in vitro* and *in vivo* findings strongly suggest that HIV-1 infection drives nuclear translocation of TRIM32, thereby affecting the stemness of NPCs.

As nuclear translocation of TRIM32 can drive c-Myc ubiquitination and HIV-1 Tat mediates translocation of TRIM32, we also looked for c-Myc ubiquitination with HIV-1

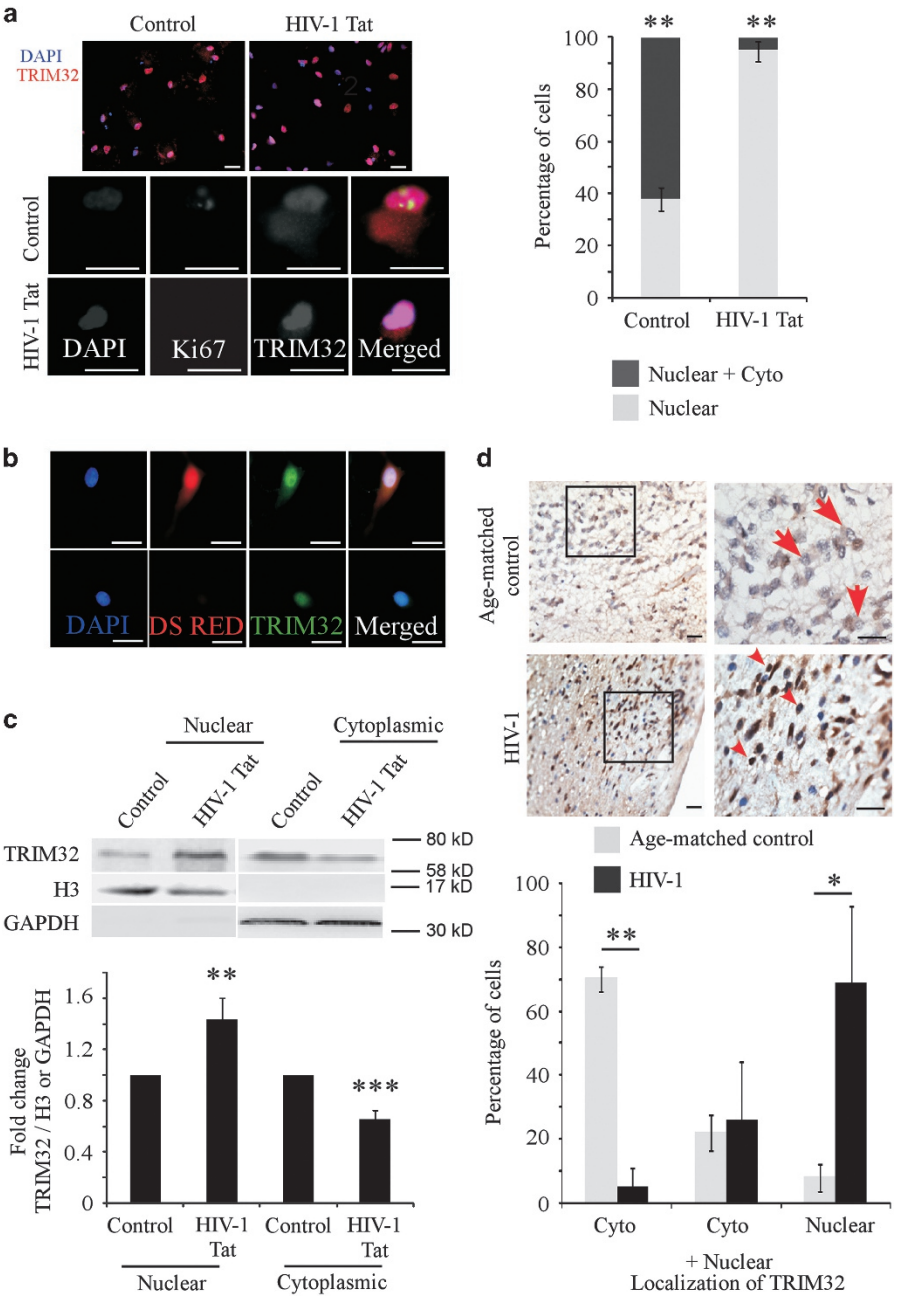

Figure 2 Nuclear translocation of TRIM32 in response to HIV-1 Tat. (**a**) Effect of HIV-1 Tat exposure (100 ng/ml) on localization of TRIM32 after 24 h; bar graph represents quantification of images; cells were counted on the basis of subcellular localization of TRIM32 that was either cytoplasmic and nuclear or nuclear only. Lower panel shows higher magnification showing localization of TRIM32 in control and HIV-1 Tat-treated hNPCs. (**b**) Localization of TRIM32 in hNPCs transfected with pDs RED-tagged HIV-1 Tat for 24 h; Tat can be visualized with Ds RED tag; scale for **a** and **b**, 20 μm. (**c**) Western blots showing fractionated nuclear and cytoplasmic levels of TRIM32 upon Tat treatment (100 ng/ml) for 24 h; quantification of band intensity is shown with bar graph, histone H3 was used as nuclear control and GAPDH as cytosolic control. (**d**) Immunohistochemical images of subventricular region of human brain of control and HIV-1-infected individuals probed for TRIM32; bar graph shows quantification of cells based on localization of TRIM32 that was either cytoplasmic, cytoplasmic and nuclear or nuclear only; arrows depict cells with cytoplasmic TRIM32 and arrowheads show cells having nuclear localization of TRIM32; scale for **d**, 50 μm. IHC data were compiled from four different controls and four different HIV-1 patients. All the other data are representative of three to five independent experiments (mean $\pm$ S.D). $^{*}P<0.05$, $^{**}P<0.005$, $^{***}P<0.0005$ with respect to control

Tat. The hNPCs were transfected with HIV-1 Tat vector, and 12 h post transfection cells were treated with MG-132 (10 μM) for 12 h and subjected to immunoprecipitation with anti c-Myc and then immunoblotted with anti-ubiquitin. Not much to our surprise, we observed increased ubiquitination with HIV-1 Tat expression in hNPCs (Supplementary Figure S4). This result further strengthened our hypothesis of HIV-1 Tat mediating proliferation arrest through c-Myc degradation.

TRIM32 is overexpressed in hNPCs due to HIV-1 Tat. Mouse NPCs overexpressing TRIM32 lose their precursor properties and commit toward neuronal lineage.[13] Hence, we

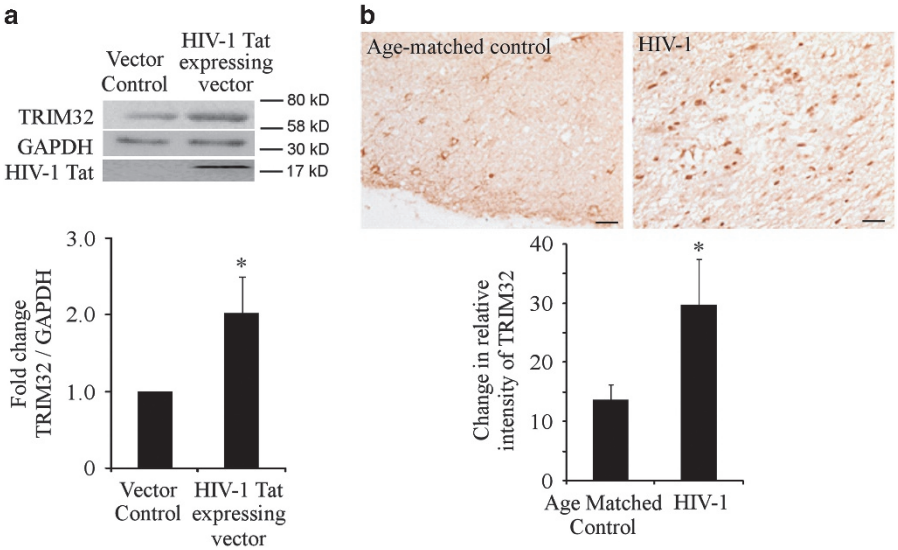

Figure 3 TRIM32 is overexpressed in hNPCs following HIV-1 Tat expression as well as in autopsy brain sections from HIV-1-infected subjects. (**a**) The hNPCs transfected with control vector or HIV-1 Tat-expressing vector; whole-cell extracts were separated through SDS-PAGE and probed for indicated antibodies; representative immunoblot showing upregulated levels of TRIM32; bar graph represents densitometric analysis of the blots, and TRIM32 levels were normalized with GAPDH. Data shown represent five independent experiments (mean ± S.D). *$P<0.05$ with respect to control. (**b**) Mean intensity analysis of TRIM32 in human brain sections. Images showing TRIM32 staining in control and HIV-1-infected human brain tissues; lower panel shows bar graph representing mean intensity analysis for control and HIV-1-infected samples. Data have been compiled from four different controls and four different HIV-1-infected subjects (mean ± S.D). *$P<0.05$ with respect to control, scale 50 μm

investigated the effect of HIV-1 Tat with treatment as well as with transient Tat transfection on expression levels of TRIM32. Cells treated with Tat showed modest but significant upregulation of 17.07% in TRIM32 levels (data not shown). To compare the effects of endogenously expressed HIV-1 Tat with that of exogenously added Tat (as the former would mimic the condition of an infected cell more closely), hNPCs were transfected with Tat-expressing vector and samples were processed for whole-cell lysate. An upregulation in TRIM32 levels (approximately twofold) was observed ($P<0.05$; Figure 3a). In order to corroborate our findings, we also analyzed mean intensity of TRIM32 in human brain sections in control as well as in infected samples particularly in SVZ area. A fold change of 2.56 was observed in TRIM32 intensity in infected cases as compared with control ($P<0.05$). As TRIM32 can potentially arrest the hNPC proliferation, it is possible that HIV-1 Tat-mediated TRIM32 overexpression may lead to proliferation arrest in these hNPCs, as shown subsequently.

Knockdown of TRIM32 reverses HIV-1 Tat-mediated proliferation arrest in hNPCs. In order to test the hypothesis of whether TRIM32 is mediating proliferation arrest in hNPCs, TRIM32 was knocked down using siRNA against TRIM32 (Figure 4a). Cells were treated with HIV-1 Tat for 24 h with or without siRNA knockdown and immunostained for Ki67. The percentage of proliferative cells in TRIM32 knockdown group was 54.2% as compared with 37.8% in the control group ($P<0.0005$). In Tat-treated group, the cell proliferation was significantly reduced to 24.2% ($P<0.005$), but TRIM32 knockdown in Tat-treated group resulted in restoration of proliferation potential back to near normal levels of 35.1% ($P<0.005$; Figure 4b). These results support our hypothesis that Tat is affecting the proliferation in hNPCs via upregulation of TRIM32 levels.

Post-transcriptional regulation of TRIM32 levels. TRIM32 mRNA transcript levels were analyzed in HIV-1 Tat-expressing hNPCs and then compared with control after 24 h of transfection. Surprisingly, we did not find any increase in transcript levels, contrary to what we observed in protein levels (Figure 5a). The rationale for this discordance could be attributed to miRNA machinery-mediated regulation. The miRNA-mediated repression leads to translational arrest of the miRNA transcript from where it can either remain repressed, degraded or even get translationally reactivated.[29] Hence, we searched for TRIM32 targeting miRNAs using miRanda database. The miR-155 and Let-7a were predicted to target TRIM32. Putative binding sites of miRNAs within TRIM32 transcript are shown (Figure 5b).

The miR-155 is altered in case of HIV-1-infected PBMCs and dendritic cells.[30,31] In addition, Let-7 family including Let-7a is observed to be downregulated in CD4+ T cells of chronically affected HIV patients.[32] As both of these microRNAs were downregulated in HIV-1 cases, they were of special interest to us and were further investigated.

In agreement with previous findings, miR-155 and Let-7a were downregulated with HIV-1 Tat expression in our model system as well. Let-7a levels were downregulated by 2.56-fold ($P<0.0005$), whereas miR-155 levels were decreased by 35% ($P<0.05$; Figure 5c).

3′UTR of TRIM32 is a potential target of miR-155. To study whether Let-7a and miR-155 bind to the 3′UTR of TRIM32 and regulate the protein levels of TRIM32, hNPCs were transfected with inhibitors/mimics of Let-7a and miR-155 and

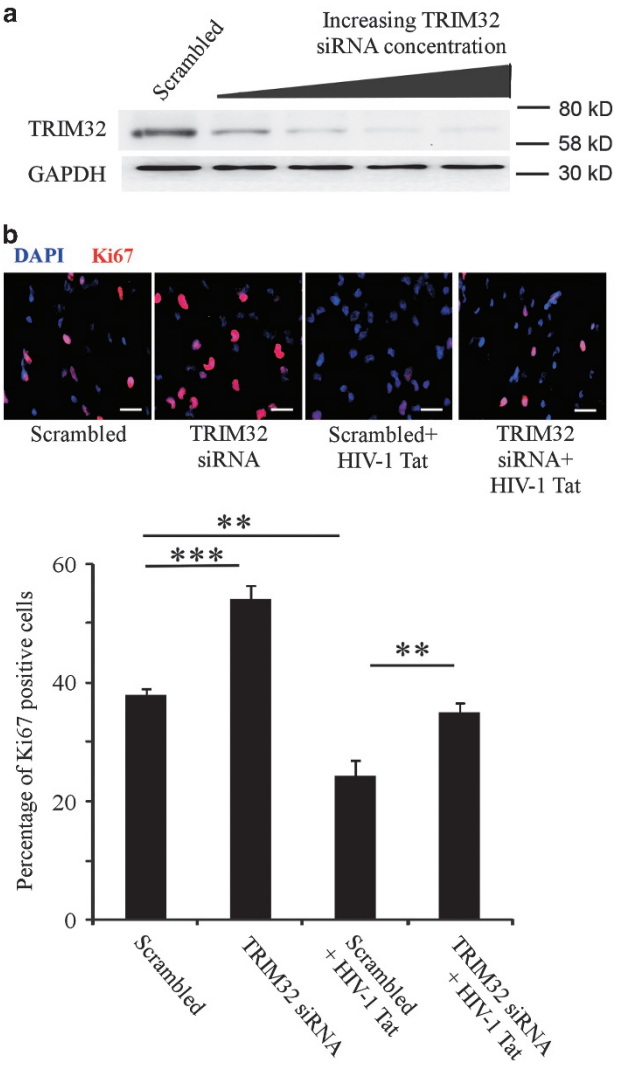

Figure 4 Knockdown of TRIM32 reverses HIV-1 Tat-mediated proliferation arrest in hNPCs (**a**) The hNPCs were transfected with siRNA against TRIM32 for 24 h; western blot showing efficacy of the knockdown in hNPCs; GAPDH was used as a loading control. (**b**) Immunocytochemistry showing Ki67 staining in hNPCs transfected with scrambled siRNA or siRNA against TRIM32 with or without Tat treatment (100 ng/ml) after 24 h; bar graph represents percentage of Ki67-positive cells in the indicated groups; transfection of siRNA against TRIM32 rescued the hNPCs from HIV-1 Tat-mediated proliferation arrest. Results are representative of four different biological replicates (mean ± S.D.). $^{**}P<0.005$, $^{***}P<0.0005$

compared with cells transfected with respective control. Samples were harvested for miRNA or whole-cell protein lysates after 24 h. Quantitative PCRs (qPCRs) were carried to check the potency of the mimic and inhibitor used (Supplementary Figure S5). Western blot analysis after transfection showed that lipofection of miR-155 inhibitor in hNPCs resulted in higher levels of TRIM32; however, Let-7a did not affect the TRIM32 levels. The miR-155 inhibition increased the TRIM32 levels up to 76.3% ($P<0.05$; Figure 6a). Similarly, transient transfection with miR-155 mimic but not Let-7a mimic lowered TRIM32 levels up to twofold ($P<0.0005$; Figure 6b), indicating that TRIM32 3′ UTR could be a direct target of miR-155. Transcript levels of TRIM32 were also analyzed with transfection of miR-155 mimic as well as miR-155 inhibitor in hNPCs but it did not show any change in the mRNA levels, and this was contrary to what we observed at the protein level (data not shown). This observation further supports our hypothesis that miR-155 is repressing the translation of TRIM32 mRNA rather than degrading it.

To further validate that TRIM32 is a potential target of miR-155 but not of Let-7a, luciferase assay was performed. 3′UTR of TRIM32 was cloned downstream of luciferase gene in pMIReporter vector (Ambion, Austin, TX, USA). Cells were transfected with pMIR TRIM32 3′UTR as well as miR-155 or Let-7a mimic. Samples were processed after 24 h of transfection. Normalized luciferase activity showed that with co-transfection of miR-155 and pMIR TRIM32 3′UTR, luciferase activity was reduced by twofold ($P<0.05$), whereas the same remains unaffected when pMIR TRIM32 3′UTR was co-transfected with Let-7a mimic (Figure 6c). These results confirmed that miR-155 targets the TRIM32 3′UTR.

MiR-155 directly regulates HIV-1 Tat-mediated proliferation arrest in hNPCs. As miR-155 suppresses TRIM32 expression and downregulation of TRIM32 induces proliferation in hNPCs, we asked whether miR-155 directly influences proliferation of hNPCs. To test the above hypothesis, cells were transfected with miR-155 mimic or inhibitor and then immunostained for Ki67 to quantify the proliferation rate. We observed that miR-155 mimic increased the proliferation from 36.5 to 47.7% ($P<0.05$), whereas inhibition of miR-155 led to a decreased rate of proliferation from 35.5% to mere 18% ($P<0.05$; Figure 7a). Hence, it can be inferred that as miR-155 regulates TRIM32 levels, increased levels of miR-155 may result in higher proliferation rate in hNPCs or vice versa.

After confirming that miR-155 regulates TRIM32 levels and can affect the proliferation of the hNPCs, we wanted to assess the effects of miR-155 in Tat-treated hNPCs. Transfection of miR-155 mimic increased the proliferation rate of hNPCs from 36.8 to 48.3% ($P<0.005$), whereas treatment of hNPCs with Tat decreased the proliferation rate to 21.4% ($P<0.005$; Figure 7b). Interestingly, in HIV-1 Tat-treated group transfected with miR-155 mimic, the proliferation was restored to 34.9% ($P<0.005$). These results further confirmed that Tat mediates its effect on TRIM32 via miR-155 dysregulation (Figure 7b).

HIV-1 infection of hNPCs induces increase in total TRIM32 levels, concomitant decrease in miR-155 level and increased nuclear translocation of TRIM32. To correlate our findings with viral infections as well, hNPCs were infected with vesicular stomatitis virus envelope G glycoprotein (VSV-G)-pseudotyped HIV-1 for 24 h and samples were processed for either total protein, miRNA assay or nuclear protein extraction. Viral infection of hNPCs resulted in 61.3% upregulation of TRIM32 levels in whole-cell protein extracts as compared with control ($P<0.005$; Figure 8a). Samples processed for miRNA assays also showed concomitant decrease of 2.38-fold in miR-155 levels in infected samples as compared with control ($P<0.05$; Figure 8b). In addition to these observations, we found that HIV-1-infected group showed an increase in nuclear levels of TRIM32 (45.2%) as compared with control ($P<0.05$; Figure 8c).

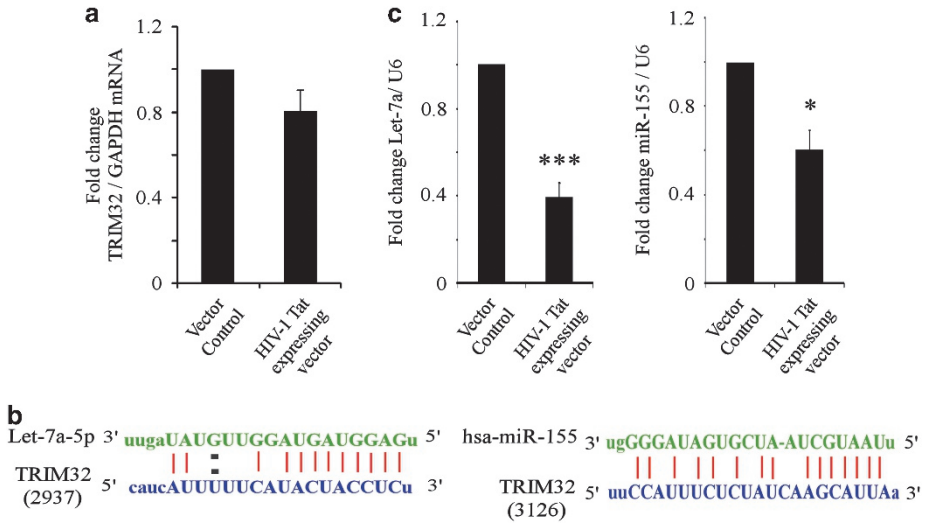

Figure 5 Post-transcriptional regulation of TRIM32 levels. (**a**) The hNPCs were transfected with control vector or HIV-1 Tat expressing vector; mRNA levels were analyzed after 24 h of transgene expression through real-time PCR; bar graph represents TRIM32 mRNA levels in indicated conditions, and GAPDH mRNA levels were used to normalize TRIM32 levels; upregulation observed at the protein levels was not observed at the mRNA levels. (**b**) miRNA binding to the 3′UTR of TRIM32 transcript is shown schematically for Let-7a and miR-155. The numbers 3126 and 2937 represent the sequence position of TRIM32 mRNA. (**c**) The hNPCs were transfected with control vector or HIV-1 Tat expressing vector for 24 h and levels of miR-155 and Let-7a were assessed through qPCR; bar graph represents levels of indicated miRNAs post transfection, and snRNA U6 was used as a normalization control. Data represent outcome of at least three independent experiments (mean ± S.D.). $^{*}P<0.05$, $^{***}P<0.0005$ with respect to control

These results further substantiated our findings and confirmed that HIV-1 infection is perhaps driving the TRIM32 upregulation and nuclear translocation in hNPCs.

Discussion

HAND is a major morbidity in HIV-1/AIDS survivors in adult and pediatric cases of neuroAIDS. This study focuses on a rather neglected aspect of neuroAIDS and unravels how HIV-1 protein Tat possibly affects self-renewing capacity of multipotent NPCs in SVZ, an important neuroanatomical area for HIV-1 infection and neurogenesis.

The effect of HIV-1 brain viremia on NPCs translates to attenuated stemness of the precursor cells interfering with human brain's regenerative capacity and contributes to HAND. To study the mechanisms leading to quiescence in NPCs, a well-characterized model of human fetal brain-derived NPCs was utilized that provided us a distinctive system to study proliferation of NPCs. Being derived from human fetal brain samples, this primary cell culture system has significant advantages over the cell lines. Our model provides a nontransformed cell system that is supposedly closer to the control physiological conditions rather than transformed cell lines derived of NPCs. Furthermore, as it is derived from human nervous tissue, this model system is apt for studies related to a human-specific virus like HIV-1 and better mimics conditions of neuroAIDS.

A recent study from our laboratory demonstrated Erk(1/2)–p21–p53 cell cycle axis is involved in the HIV-1 Tat-mediated proliferation arrest of precursor cells.[33] The mechanism by which HIV-1 Tat disturbs normal functionality of NPCs is still unclear. Henceforth, the role of TRIM32 (a neural stem cell determinant and HIV-1 Tat interacting partner) was questioned in the HIV-1 Tat-induced quiescence in hNPCs.

TRIM32 translocates to the nucleus upon neurogenesis signal where it ubiquitinates c-myc that results in its proteasomal-mediated degradation.[14] TRIM32 thereby arrests the proliferation of neural stem cells upon translocation into the nucleus, laying groundwork for initiation for neurogenesis. We observed that TRIM32 localization was perturbed by HIV-1 Tat where increased trafficking of TRIM32 molecules into the nucleus was observed to be closely associated with HIV-1 Tat. To validate the findings of our *in vitro* observations, we utilized human brain tissues from HIV-1-infected individuals and reconfirmed the increased nuclear translocation of TRIM32 molecules in the SVZ area of diseased brain tissues. Increased nuclear trafficking of TRIM32 leads to degradation of c-myc, contributing to arrested proliferation of NPCs mediated by HIV-1 Tat. This was further confirmed with our experiments showing enhanced c-Myc ubiquitination with HIV-1 Tat in hNPCs. The mechanism of nuclear translocation of TRIM32 is unknown. As TRIM32 does not contain any classical nuclear localization signal, post-translation modification such as ubiquitination is predicted to be a signal for entry into the nucleus.[14] Perhaps, HIV-1 Tat promotes such modifications that mediate entry of TRIM32 into the nucleus. Another possible mechanism could be of direct pull of TRIM32 into the nucleus through interaction with HIV-1 Tat, as this viral protein has competent NLS signal. It will be an interesting query to address the mechanisms that HIV-1 Tat exploits to induce increased trafficking of TRIM32 molecules into the nucleus.

Overexpression of TRIM32 in NPCs is related to their attenuated proliferation.[13] When a neural stem cell undergoes mitosis, enrichment of TRIM32 in the daughter cell decides the fate of the progeny. Following asymmetric division of a mouse neural precursor cells, TRIM32 accumulation in one of the progenies causes it to commit toward neuronal lineage,

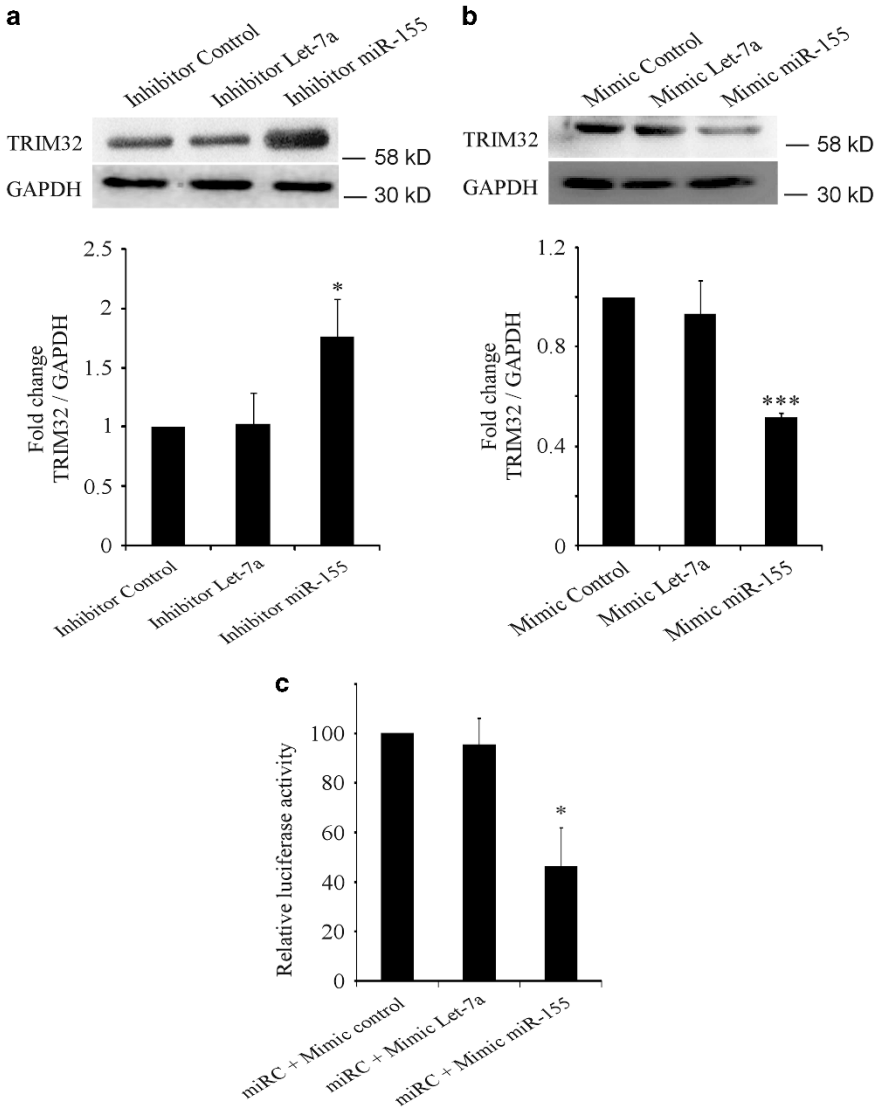

Figure 6 3′UTR of TRIM32 is a potential target of miR-155. The hNPCs were transfected for 24 h with (**a**) inhibitor and (**b**) mimic of the indicated miRNAs with their respective control. Western blots showing TRIM32 levels after transfection; lower panels show densitometric analysis of the blots. (**c**) miReporter TRIM32 3′UTR was transfected with mimic control, miR-155 or Let-7a mimic in HeLa cells for 24 h; bar graph represents normalized luciferase activity in the indicated groups. All experiments were repeated at least three times (mean ± S.D.). $^{*}P<0.05$, $^{***}P<0.0005$ with respect to control

whereas the other progeny that has inherited lesser number of TRIM32 molecules retains its precursor fate. We observed higher expression of TRIM32 protein induced by HIV-1 Tat that possibly mediated proliferation arrest. We further observed increased relative intensity in TRIM32 levels in human brain sections in HIV-1 cases as compared with control. This hypothesis was further validated by TRIM32 knockdown in HIV-1 Tat-treated groups wherein HIV-1 Tat-mediated proliferation arrest in hNPCs was inhibited.

Interestingly, we also observed lack of increase at the transcript levels of TRIM32 following HIV-1 Tat exposure and subsequently proved that RNAi-mediated gene silencing is involved in regulating TRIM32 protein levels. The role of microRNA (miR-155) in regulation of 3′UTR of the TRIM32 transcripts was elucidated through mimic/knockdown strategies and luciferase reporter assays. Furthermore, evidence for the role of miR-155 in regulation of proliferation of hNPCs was also demonstrated. In addition, miR-155 could directly rescue the hNPCs from HIV-1 Tat-mediated proliferation arrest. Dysregulation of miR-155 is associated with aberrant proliferation in different tissues.[34–37] Enhanced expression of miR-155 leads to enhanced proliferation, whereas downregulated levels of miR-155 is linked with decreased proliferation in various tissues. MiR-155 knockdown has been reported to decrease proliferation in glioblastomas.[38] However, literature showing role of miR-155 in the dysregulation of stemness of hNPCs was lacking till this study. MiR-155 negatively regulates SOX6 expression that positively influences the expression of p21 in hepatocellular carcinoma.[37] Enhanced levels of p21 have been reported in case of HIV-1 Tat-mediated proliferation arrest[33] that would possibly suggest that declined levels of miR-155 might upregulate SOX6 and

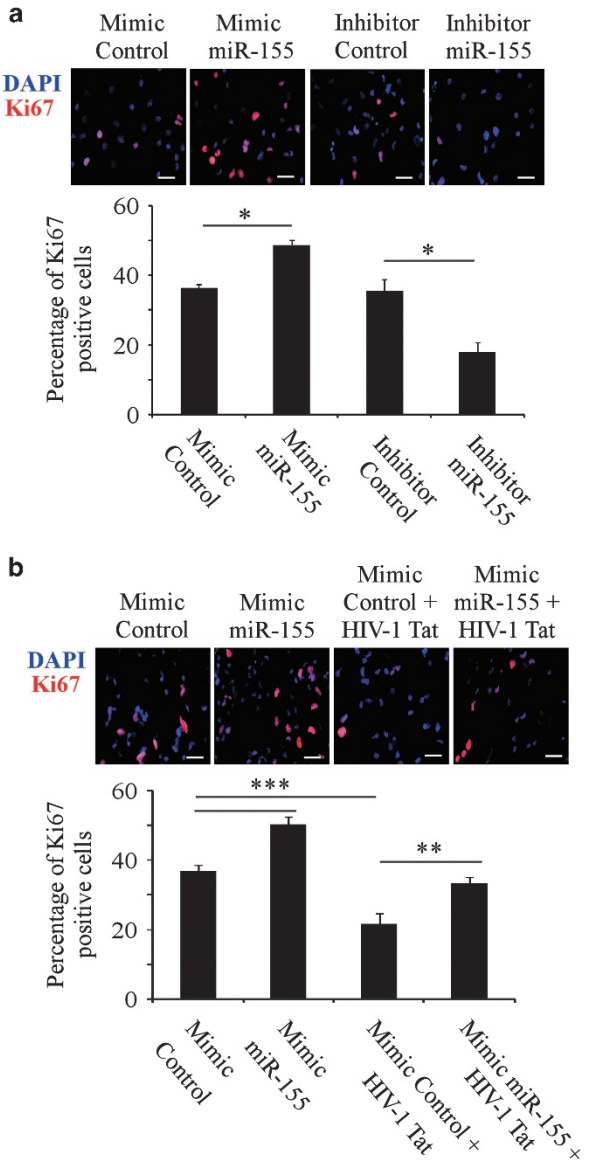

Figure 7 MiR-155 directly regulates HIV-1 Tat-mediated proliferation arrest in hNPCs. (**a**) The hNPCs were transfected for 24 h with mimic control, inhibitor control, mimic miR-155 or inhibitor miR-155; immunocytochemistry images showing Ki67 staining in the indicated groups; lower panel shows bar graph that represents the percentage of Ki67-positive cells in the indicated groups. (**b**) The hNPCs were transfected with mimic control or mimic miR-155 with or without HIV-1 Tat (100 ng/ml) for 24 h; immunocytochemistry images showing Ki67-positive cells; lower panel shows bar graph representing percentage of Ki67-positive cells in the indicated groups. All experiments were repeated at least three times (mean ± S.D.); $^{*}P<0.05$, $^{**}P<0.005$, $^{***}P<0.0005$

result in HIV-1 Tat-induced enhancement in p21 expression in hNPCs. If and how SOX6 is regulated by TRIM32 is another open question.

The role of TRIM32 and HIV-1 Tat interaction in post-transcriptional regulation of TRIM32 is another interesting query. TRIM32 is an Argonaute interacting protein. It interacts with three Argonaute proteins, Ago-1, Ago-2 and Ago-3.[39] Hence, TRIM32 can be regarded as RISC interacting protein. NHL domain of TRIM32 is reported to influence miRNA activity.[13] Enhanced activity of a microRNA biomolecule could be a result of enhanced transcription or enhanced processing to form a functionally mature miRNA. How TRIM32 activates miRNAs is not known but NHL domain of TRIM32 has been implicated to influence the miRNA activation. HIV-1 Tat interacts with the same NHL domain of TRIM32; NHL domain perhaps when hijacked by HIV-1 Tat culminates into down-regulated levels of miR-155. Another possibility is Tat somehow independently disrupts biogenesis of mature miR-155 and results in downregulated levels of miR-155 levels and hence ensuing enhanced TRIM32 protein levels.

As HIV-1 Tat was attenuating the proliferation, it was questioned whether Tat was inducing any lineage commitment (glial or neuronal). With acute HIV-1Tat exposure, we observed that Tat did not enhance commitment of hNPCs toward any lineage (Supplementary Figure S6). The above observation indicated that hNPCs were merely quiescent with HIV-1 Tat exposure. In fact, TRIM32 knockdown in HIV-1 Tat-treated hNPCs readily restored the proliferation.

To further strengthen our findings, we infected hNPCs with VSV-G-pseudotyped HIV-1 and found similar observations of increased whole-cell TRIM32 levels, concomitant decrease in miR-155 levels and increase in nuclear translocation of TRIM32 with HIV-1 infection.

TRIM32 overexpression has been linked to enhanced commitment toward neuronal lineage.[13] On the other hand, HIV-1 Tat represses commitment toward neuronal lineage.[9] TRIM32 utilizes different domains to execute its diverse functions; for example, the one it utilizes to control proliferation might not be the same it uses to induce neuronal differentiation. Hence, it would be interesting to investigate how HIV-1 Tat induces TRIM32 overexpression yet hinders neurogenesis, what are the pathways that TRIM32 overexpression triggers and the mechanism of interference of HIV-1 Tat with these molecular switches resulting into aberrant neurogenesis; these lines of investigation are being currently pursued in our laboratory.

The data shown here assert that proliferation arrest in primary culture of hNPCs because of HIV-1 Tat can be rescued through TRIM32 knockdown that could be either mediated by a siRNA against TRIM32 or miR-155 mimic. We hereby report a novel molecular cascade consisting of miR-155 and TRIM32 involved in HIV-1 Tat-mediated quiescence in hNPCs and show how the virus exploits the microRNA machinery to induce proliferation arrest in hNPCs.

Materials and Methods

The hNPC isolation. Handling of human tissues was carried out in strict accordance with the guidelines of Institutional Human Ethics Committee and Stem Cell and Research Committee of National Brain Research Centre, India, and the Indian Council of Medical Research (ICMR), India. The hNPCs were isolated from the telencephalon region of 10–15-week-old fetuses as described earlier.[9] Isolated cells were cultured in Poly D-lysine (Sigma-Aldrich, St. Louis, MO, USA)-coated flasks in Neurobasal media (Invitrogen, San Diego, CA, USA) supplemented with Neural Survival Factor-1 (Lonza, Charles City, IA, USA), N2 supplement (Invitrogen), 25 ng/ml bovine fibroblast growth factor (bFGF) (Sigma-Aldrich) and 20 ng/ml epidermal growth factor (EGF) (Sigma-Aldrich). Cells were passaged 9–10 times and then utilized for experiments after their characterizations. These NPCs were tested for the expression of Nestin and SOX2 positivity (marker for stemness), which was found to be >99%, and the NPCs were negative for any lineage-specific markers particularly glial fibrillary acidic protein (GFAP) or microtubule-associated protein 2 (MAP2). Their potential as neural stem cell was assessed by their ability to

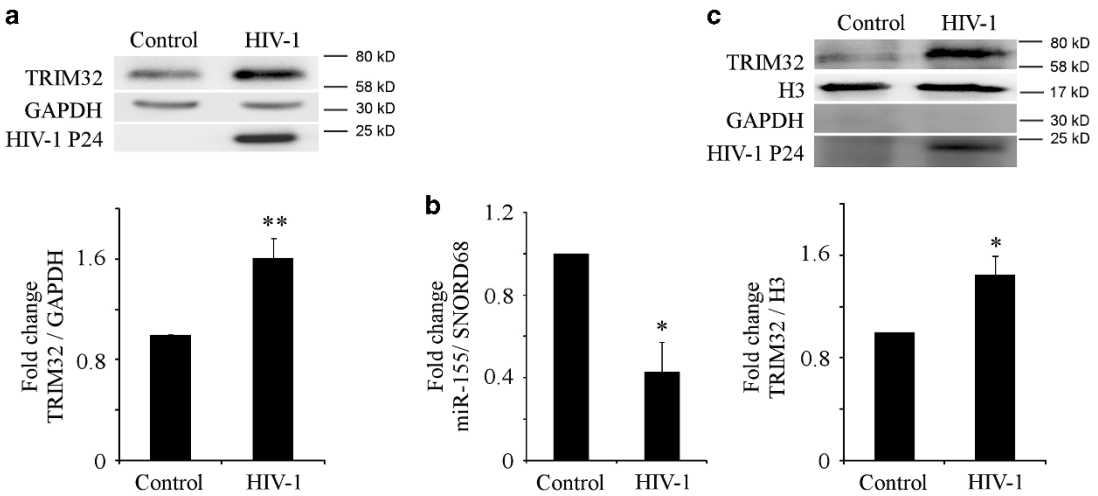

Figure 8 Infection of human neural precursor cells. The hNPCs were infected with VSV-G-pseudotyped HIV-1 for 24 h. (**a**) Western blots showing upregulated levels of TRIM32 upon HIV-1 infection; GAPDH was used as normalization control, and lower panel shows densitometric analysis for the same. (**b**) Bar graph showing miR-155 levels in hNPCs upon HIV-1 infection. (**c**) Western blots showing TRIM32 levels in nuclear extracts with HIV-1 infection; H3 was used as a normalization control, and lower panel shows densitometric analysis of the blots. All experiments were repeated at least three times (mean ± S.D.); $^{*}P<0.05$, $^{**}P<0.005$

form neurospheres and differentiate into neurons or astrocytes (analyzed by Tuj-1 and GFAP positivity). NPCs were differentiated into neuronal lineage by removing bFGF and EGF from the above mentioned media cocktail and supplementing the same with platelet-derived growth factor (PDGF) (Sigma-Aldrich) and brain-derived neurotrophic factor (BDNF) (Sigma-Aldrich). NPCs were differentiated into astrocytes by replacing the NPC media with minimum essential medium (MEM) (Sigma-Aldrich) supplemented with 10% fetal bovine serum (Sigma-Aldrich). For both neuronal and astrocytic lineage, differentiation was carried out for 21 days. Depending upon exposure to defined media conditions, >95% of the differentiated cells were either Tuj-1 or GFAP positive (Supplementary Figure S1).

Immunohistochemistry of human brain sections. Paraffin-processed 5 μm serial sections of control (non-HIV infected ($n=4$)) and HIV-1 infected without associated opportunistic infections ($n=4$) were obtained from Human Brain Tissue Repository, National Institute of Mental Health and Neurosciences, Bangalore, India. Age-matched controls and HIV-1-infected tissues from the frontal cortex–basal ganglia that included the lateral ventricle with SVZ were used in the study (age range: 34–40 years). In addition, a 23-week-old fetal tissue was included in the study to compare the observations with that of adult control tissues. The control brain sections were from cases of accidental death who succumbed to road traffic accidents, who had no prior history of neurological illness and who did not reveal any pathology other than related to trauma. Tissue sections were deparaffinized by immersing in xylene, followed by increasing grades of alcohol. Sections were treated with methanol containing 3% hydrogen peroxidase for quenching endogenous peroxidase activity, followed by antigen retrieval with sodium citrate buffer (pH 6.0). Sections were blocked using Power Block (BioGenex, Fremont, CA, USA). Anti-Nestin (Santa Cruz Biotechnology, Santa Cruz, TX, USA; 1 : 50) and anti-TRIM32 (Novus Biologicals, Littleton, CO, USA; 1 : 250) were used to detect the respective antigens with overnight incubations at 4 °C. One-step Polymer-HRP Detection System (BioGenex) was used to develop the staining. Sections were imaged under Olympus BX51 (Tokyo, Japan). Images from 8 to 10 random fields were captured from SVZ region for quantification.

For measurement of TRIM32 intensity in human brain sections in SVZ area, acquired images were converted to 8-bit grayscale. Intensity of the staining was assessed by determining mean pixel density by using ImageJ software (NIH, Bethesda, MD, USA). Background staining was subtracted from the mean density obtained. All intensity measurements were performed by a person blinded to experimental groups.

HIV-1 Tat treatment and HIV-1 Tat transient expression. Recombinant HIV-1 Tat Clade B (Diatheva, Fano, Italy) was used for treatment of hNPCs at a concentration of 100 ng/ml for 24 h. The concentration of HIV-1 Tat chosen was in line with the existing literature that showed the effect of HIV-1 Tat on proliferation of NPCs,[9,33,40] and is consistent with other studies.[41–44] Full-length HIV-1 Tat-expressing pcDNA 3.1 vector and pDS RED was a kind gift from Professor Udaykumar Ranga (JNCASR, Bangalore, India). The plasmids were transfected in 80% confluent hNPCs using Lipofectamine 2000 (Invitrogen) according to the manufacturer's protocol. Transfected cells were processed either for mRNA, miRNA or protein isolation according to the requirement of the experiments.

Immunocytochemistry. For immunocytochemistry, experiments were carried out in eight-well chamber slides (Nunc, Kamstrupvej, Denmark). The hNPCs were plated at a density of 20 000 cells per well. Cells were fixed for 20 min with 4% paraformaldehyde, washed thrice with PBS, blocked and permeabilized using 10% normal goat serum (Vector Labs, Burlingame, CA, USA) or 4% bovine serum albumin (BSA) containing 0.5% Triton X-100. Cells were incubated with the following primary antibodies overnight at 4 °C: anti-Ki67 (Novacastra, Wetzlar, Germany; 1 : 1000) and/or anti-TRIM32 (Gramsch Laboratories, Schwabhausen, Germany; 1 : 250), Tuj-1 (Promega, Madison, WI, USA; 1 : 3000), DCX (Abcam, Cambridge, UK, 1 : 1000) and GFAP (Dako, Glostrup, Denmark; 1 : 1000 and Santa Cruz Biotechnology; 1 : 200). Later, the cells were washed thrice after incubation with primary antibody and incubated with appropriate secondary antibodies tagged with Alexa Flour 594 and Alexa Flour 488 (Invitrogen). Slides were mounted with Hard set mounting media containing DAPI (Vector Labs). For each group, 5–7 images were captured from random fields. Images were acquired using AxioImager.Z1 microscope (Carl Zeiss, Heidenheim, Germany).

Small interfering RNA-mediated knockdown of TRIM32: for TRIM32 knockdown. Endoribonuclease-prepared siRNAs (esiRNAs) against TRIM32 (Sigma-Aldrich) was used. A total of 1 pmol of esiRNA was transfected using RNAi Max (Invitrogen) according to the manufacturer's instructions. MISSION siRNA Universal Negative Control 1 (Sigma-Aldrich) was used as scrambled control. To check the efficiency of the knockdown at protein level, concentrations of 2.5, 5, 10 and 20 pmol were used. Then, 10 pmol concentration was selected as it showed highest level of knockdown of TRIM32 and was scaled down 10 times accordingly for experiments that were carried out in eight-well chamber slides. Samples were processed for immunocytochemistry after 24 h of transfection.

Preparation of protein extracts and western blotting. Samples were processed for either whole-cell extract or nuclear and cytoplasmic extract. Whole-cell extract buffer consisted of 1% Triton X-100, 150 mM NaCl, 10 mM Tris-HCl (pH 8.0), 5 mM EDTA (pH 8.0), 1 mM EGTA (pH 8.0), 0.5% NP-40, 50 mM sodium fluoride, 1 mM sodium orthovanadate and protease inhibitor cocktail (Roche, Mannheim, Germany). The cytosolic extraction buffer comprised 0.2% Triton X-100,

HEPES buffer (pH 7.6), 10 mM magnesium chloride, 100 mM potassium chloride, 10 mM sodium butyrate and protease inhibitor cocktail. Cells were lysed with the cytosolic extraction buffer and then centrifuged. Pellet so obtained was lysed with nuclear extraction buffer that contained 50 mM Tris (pH 7.5), 150 mM sodium chloride, 50 mM sodium fluoride, 1 mM EDTA, 1 mM sodium orthovendate, 2% sodium dodecyl sulfate and protease inhibitor cocktail. Protein concentration was estimated by bicinchoninic acid (Sigma-Aldrich) and 4% copper sulfate. Protein extract was separated on 12% SDS-PAGE and then blotted onto nitrocellulose membrane (MDI, Ambala, India). The membranes were blocked with 5% skimmed milk or 10% normal goat serum (Vector Labs) in PBS/Tween-20. Blots were incubated overnight at 4 °C with the following primary antibodies: TRIM32 (Gramsch Laboratories; 1 : 2000), GAPDH (Santa Cruz Biotechnology; 1 : 10 000), histone H3 (Millipore, Bedford, MA, USA; 1 : 3000), anti-HIV-1 Tat (a kind gift from Professor Udaykumar Ranga, JNCASR; 1 : 4000) and anti-p24 monoclonal antibody (NIH AIDS Reagent Programme, Germantown, MD, USA; 1 : 3000). After 3 washes with TBS/Tween-20 (TBST), blots were probed with HRP-conjugated secondary antibodies (Vector Labs) for 1 h. Later, blots were washed thrice with TBST and developed with chemiluminescence reagent (Millipore, Billerica, MA, USA). Blots were imaged using ChemiGenius Bio-imaging System (Syngene, Cambridge, UK). Densitometric analysis of the protein bands were carried out using ImageJ software (NIH).

Quantitative real-time PCR. RNA was extracted from the samples using TRIZOL (Sigma-Aldrich) according to the manufacturer's protocol. cDNA was synthesized from the extracted RNA using high-capacity cDNA reverse transcription kit (Applied Biosystems, Austin, TX, USA) in accordance with the manufacturer's instructions. Real-time detection was performed with SYBER Green master mix (Applied Biosystems) using following primers for TRIM32 and GAPDH: TRIM32 forward 5′-GGCCACTGTACACTCCCTGT-3′ and TRIM32 reverse 5′-AGCCAAAGA GCCTGTGAAGA-3′, GAPDH forward 5′-GAAGGTGAAGGTCGGAGTC-3′ and GAPDH reverse 5′-GAAGATGGTGATGGGATTTC-3′. The cycling conditions used were 95 °C for 3 min (1 cycle), 95 °C for 20 s, 62 °C for 30 s and 72 °C for 40 s (35 cycles).

For miRNA isolation, RNA was isolated from the cells using miRNAeasy mini kit (Qiagen, Hilden, Germany). cDNA was synthesized using miScript II RT kit (Qiagen) according to the manufacturer's protocol. Specific primers for miR-155-5p and Let-7a-5p (Qiagen) were used to detect the respective miRNAs. qPCR was performed to detect the levels of miRNAs of interest using miScript SYBER Green PCR kit (Qiagen) as per the manufacture's protocol. qPCR was carried out using ROTOR-GENE Q (Qiagen). Specificity of all the primers used was confirmed with single product peak in the melt curve analysis.

miRNA mimic and inhibitor transfection. The hNPCs were plated at 80% confluency in T25 flasks. Then, 100 pmol of Syn-hsa-miR-155-5p miScript miRNA mimic or Syn-hsa-Let-7a-5p miScript miRNA mimic (Qiagen) was used to transfect hNPCs. All Stars Negative Control siRNA (Qiagen) was used as a mimic control. Next, 100 pmol of Anti-hsa-miR-155-5p (Qiagen) and Anti-hsa-Let-7a-5p (Qiagen) were transfected in hNPCs to inhibit respective miRNAs. miScript Inhibitor Negative Control (Qiagen) was used as control for miRNA inhibition experiments. Transfections were performed using RNAi MAX (Invitrogen). Opti-MEM (Invitrogen) was used as transfection media. Cells were replaced with normal media after 4 h of transfection and samples were processed for protein extraction after 24 h. For immunocytochemistry assays of miR-155 mimic and inhibitor that was carried out in eight-well chamber slides, concentrations of the mimic and the inhibitor was scaled down 10 times accordingly. Efficacy of miRNA mimic and inhibition was checked through qPCR using primers of respective miRNAs.

miRNA target prediction. The miRanda database (www.microrna.org) was used to predict the miRNAs targeting TRIM32 3′UTR.

Cloning of TRIM32 3′UTR and Luciferase assay. 3′UTR of TRIM32 was amplified using given primers: forward 5′-CAGTCTGATCGTCTTTACCAGTATG-3′ and reverse 5′-ATCCAAAGAAACACTACTACCATAAAAA-3′. The 1037 bp long amplified product contained the predicted miR-155 binding site and was cloned in pMIR-Reporter (Ambion). The product was cloned between *Spe*I and *Hin*dIII restriction sites downstream of the luciferase coding region.

The TRIM32 3′UTR luciferase reporter was transfected in HeLa cells with or without miR-155 or Let-7a mimic. Then, 5 μg of the cloned product and 100 pmol of the mimic were used to transfect the cells using Lipofectamine 2000 as per the manufacturer's protocol. Samples were collected for luciferase detection after 24 h. Luciferase activity was measured with a Luciferase detection kit (Promega) as per the manufacturer's protocol. Detection was performed using Sirius single tube luminometer (Berthold Detection Systems, Pforzheim, Germany) and Luciferase units were normalized with the total protein.

HIV-1 infection of hNPCs. Viral stocks of VSV-G)-psuedotyped HIV-1 were prepared by co-transfection of pNL4-3 and VSV-G expressing plasmid into HEK 293T cells using Lipofectamine 2000 (Invitrogen). Medium was replaced with fresh complete DMEM 6 h post transfection. The supernatant containing virus particles was collected 48 h post transfection. The collected virus supernatant was filtered through a 0.45 μm pore size filter and the aliquots were then stored in − 80 °C. P24 assay for viral titer was done by β-galactosidase staining of HIV-1 using TZM-bl reporter cell line.

HNPCs were infected with VSV-G-psuedotyped HIV-1 for 4 h at 37 °C by incubating the cells with equal amounts of infectious virus (1 MOI) assessed by β-galactosidase staining using HIV-1 indicator TZMbl cells. The infected cells were harvested at 24 h post infection and subjected to protein isolation or miRNA assay.

Ubiquitination assay. Human neural precursor cells were transfected with HIV-1 Tat vector and Ubiquitin expressing vector (a kind gift from Dr. A Banerjea, NII, New Delhi, India) using Lipofectamine 2000 (Invitrogen) following the manufacturer's instructions. After 12 hours of transfection, MG-132 (Calbiochem, Merck Millipore, Billerica, MA, USA; 10 μM) was added to the media and cells were harvested after 12 h. Whole-cell extracts were prepared and 500 μg of protein was incubated overnight with anti-c-myc (Santa Cruz Biotechnology). Antigen antibody complexes were pulled out by incubating the lysate with Sepharose G beads (GE Healthcare, Buckinghamshire, UK). Beads were washed 6 times with IP buffer. Immunoprecipitated protein was then separated on 8% SDS-PAGE gel and blot was probed with anti-ubiquitin (Dako) to detect ubiquitinated species of c-Myc. Input used was 20% of the lysate used in IP.

Statistical analysis. Data are represented as mean $\pm$ S.D. All experiments were carried out three to five times independently. Significance of the comparison between control and treated groups was computed using Student's *t*-test. $P < 0.05$ was considered as statistically significant.

Conflict of Interest

The authors declare no conflict of interest.

Acknowledgements. Technical assistance from Ms. Rabia Khatoon, Mr. DL Meena and Mr. Naushad Alam of NBRC, India, and Mr. Shivshankar HN, Neuromuscular Laboratory, NRC, NIMHANS, India, during the study is greatly acknowledged. Availability of well-characterized autopsy brain sections from Human Brain Tissue Repository for Neurobiological Studies, Department of Neuropathology, National Institute of Mental Health and Neurosciences, Bangalore, India, is greatly appreciated. We also acknowledge Mr. Bharat Prajapati, NBRC, for critical analysis of the manuscript. Senior Research Fellowship to Ms. Mahar Fatima from CSIR, New Delhi, India, and project assistantship to Ms Rina Kumari from National Brain Research Centre, Manesar, India, are greatly acknowledged. Financial support for the study from NBRC core funds to PS is greatly acknowledged. This project in the lab of JCS is supported by the Schram-Stiftung (T287/21795/2011) and the Boehringer Ingelheim Foundation.

1. Maschke M, Kastrup O, Esser S, Ross B, Hengge U, Hufnagel A. Incidence and prevalence of neurological disorders associated with HIV since the introduction of highly active antiretroviral therapy (HAART). *J Neurol Neurosurg Psychiatry* 2000; **69**: 376–380.
2. Neuenburg JK, Brodt HR, Herndier BG, Bickel M, Bacchetti P, Price RW *et al.* HIV-related neuropathology, 1985 to 1999: rising prevalence of HIV encephalopathy in the era of highly active antiretroviral therapy. *J Acquir Immune Defic Syndr* 2002; **31**: 171–177.
3. Zhou L, Saksena NK. HIV associated neurocognitive disorders. *Infect Dis Rep* 2013; **5**: e8.
4. Langford D, Marquie-Beck J, de Almeida S, Lazzaretto D, Letendre S, Grant I *et al.* Relationship of antiretroviral treatment to postmortem brain tissue viral load in human immunodeficiency virus-infected patients. *J Neurovirol* 2006; **12**: 100–107.
5. Kramer-Hammerle S, Rothenaigner I, Wolff H, Bell JE, Brack-Werner R. Cells of the central nervous system as targets and reservoirs of the human immunodeficiency virus. *Virus Res* 2005; **111**: 194–213.

6. Rothenaigner I, Kramer S, Ziegler M, Wolff H, Kleinschmidt A, Brack-Werner R. Long-term HIV-1 infection of neural progenitor populations. *AIDS* 2007; **21**: 2271–2281.
7. Schwartz L, Civitello L, Dunn-Pirio A, Ryschkewitsch S, Berry E, Cavert W *et al.* Evidence of human immunodeficiency virus type 1 infection of nestin-positive neural progenitors in archival pediatric brain tissue. *J Neurovirol* 2007; **13**: 274–283.
8. Lawrence DM, Durham LC, Schwartz L, Seth P, Maric D, Major EO. Human immunodeficiency virus type 1 infection of human brain-derived progenitor cells. *J Virol* 2004; **78**: 7319–7328.
9. Mishra M, Taneja M, Malik S, Khalique H, Seth P. Human immunodeficiency virus type 1 Tat modulates proliferation and differentiation of human neural precursor cells: implication in NeuroAIDS. *J Neurovirol* 2010; **16**: 355–367.
10. Okamoto S, Kang YJ, Brechtel CW, Siviglia E, Russo R, Clemente A *et al.* HIV/gp120 decreases adult neural progenitor cell proliferation via checkpoint kinase-mediated cell-cycle withdrawal and G1 arrest. *Cell Stem Cell* 2007; **1**: 230–236.
11. Schwartz L, Major EO. Neural progenitors and HIV-1-associated central nervous system disease in adults and children. *Curr HIV Res* 2006; **4**: 319–327.
12. Fridell RA, Harding LS, Bogerd HP, Cullen BR. Identification of a novel human zinc finger protein that specifically interacts with the activation domain of lentiviral Tat proteins. *Virology* 1995; **209**: 347–357.
13. Schwamborn JC, Berezikov E, Knoblich JA. The TRIM-NHL protein TRIM32 activates microRNAs and prevents self-renewal in mouse neural progenitors. *Cell* 2009; **136**: 913–925.
14. Hillje AL, Worlitzer MM, Palm T, Schwamborn JC. Neural stem cells maintain their stemness through protein kinase C zeta-mediated inhibition of TRIM32. *Stem Cells* 2011; **29**: 1437–1447.
15. Hillje AL, Pavlou MA, Beckmann E, Worlitzer MM, Bahnassawy L, Lewejohann L *et al.* TRIM32-dependent transcription in adult neural progenitor cells regulates neuronal differentiation. *Cell Death Dis* 2013; **4**: e976.
16. Versteeg GA, Rajsbaum R, Sanchez-Aparicio MT, Maestre AM, Valdiviezo J, Shi M *et al.* The E3-ligase TRIM family of proteins regulates signaling pathways triggered by innate immune pattern-recognition receptors. *Immunity* 2013; **38**: 384–398.
17. Carthagena L, Bergamaschi A, Luna JM, David A, Uchil PD, Margottin-Goguet F *et al.* Human TRIM gene expression in response to interferons. *PLoS One* 2009; **4**: e4894.
18. Ozato K, Shin DM, Chang TH, Morse HC 3rd. TRIM family proteins and their emerging roles in innate immunity. *Nat Rev Immunol* 2008; **8**: 849–860.
19. Rahm N, Telenti A. The role of tripartite motif family members in mediating susceptibility to HIV-1 infection. *Curr Opin HIV AIDS* 2012; **7**: 180–186.
20. Uchil PD, Hinz A, Siegel S, Coenen-Stass A, Pertel T, Luban J *et al.* TRIM protein-mediated regulation of inflammatory and innate immune signaling and its association with antiretroviral activity. *J Virol* 2013; **87**: 257–272.
21. Zhang J, Hu MM, Wang YY, Shu HB. TRIM32 protein modulates type I interferon induction and cellular antiviral response by targeting MITA/STING protein for K63-linked ubiquitination. *J Biol Chem* 2012; **287**: 28646–28655.
22. Frosk P, Weiler T, Nylen E, Sudha T, Greenberg CR, Morgan K *et al.* Limb-girdle muscular dystrophy type 2H associated with mutation in TRIM32, a putative E3-ubiquitin-ligase gene. *Am J Hum Genet* 2002; **70**: 663–672.
23. Locke M, Tinsley CL, Benson MA, Blake DJ. TRIM32 is an E3 ubiquitin ligase for dysbindin. *Hum Mol Genet* 2009; **18**: 2344–2358.
24. Horn EJ, Albor A, Liu Y, El-Hizawi S, Vanderbeek GE, Babcock M *et al.* RING protein Trim32 associated with skin carcinogenesis has anti-apoptotic and E3-ubiquitin ligase properties. *Carcinogenesis* 2004; **25**: 157–167.
25. Yokota T, Mishra M, Akatsu H, Tani Y, Miyauchi T, Yamamoto T *et al.* Brain site-specific gene expression analysis in Alzheimer's disease patients. *Eur J Clin Invest* 2006; **36**: 820–830.
26. Ruan CS, Wang SF, Shen YJ, Guo Y, Yang CR, Zhou FH *et al.* Deletion of TRIM32 protects mice from anxiety- and depression-like behaviors under mild stress. *Eur J Neurosci* 2014; **40**: 2680–2690.
27. Sato T, Okumura F, Kano S, Kondo T, Ariga T, Hatakeyama S *et al.* TRIM32 promotes neural differentiation through retinoic acid receptor-mediated transcription. *J Cell Sci* 2011; **124**: 3492–3502.
28. Krathwohl MD, Kaiser JL. HIV-1 promotes quiescence in human neural progenitor cells. *J Infect Dis* 2004; **190**: 216–226.
29. Wilczynska A, Bushell M. The complexity of miRNA-mediated repression. *Cell Death Differ* 2015; **22**: 22–33.
30. Sun G, Li H, Wu X, Covarrubias M, Scherer L, Meinking K *et al.* Interplay between HIV-1 infection and host microRNAs. *Nucleic Acids Res* 2012; **40**: 2181–2196.
31. Napuri J, Pilakka-Kanthikeel S, Raymond A, Agudelo M, Yndart-Arias A, Saxena SK *et al.* Cocaine enhances HIV-1 infectivity in monocyte derived dendritic cells by suppressing microRNA-155. *PLoS One* 2013; **8**: e83682.
32. Swaminathan S, Suzuki K, Seddiki N, Kaplan W, Cowley MJ, Hood CL *et al.* Differential regulation of the Let-7 family of microRNAs in CD4+ T cells alters IL-10 expression. *J Immunol* 2012; **188**: 6238–6246.
33. Malik S, Saha R, Seth P. Involvement of extracellular signal-regulated kinase (ERK1/2)-p53-p21 axis in mediating neural stem/progenitor cell cycle arrest in co-morbid HIV-drug abuse exposure. *J Neuroimmune Pharmacol* 2014; **9**: 340–353.
34. Zhang CM, Zhao J, Deng HY. MiR-155 promotes proliferation of human breast cancer MCF-7 cells through targeting tumor protein 53-induced nuclear protein 1. *J Biomed Sci* 2013; **20**: 79.
35. Li T, Yang J, Lv X, Gao C, Xing Y, Xi T. miR-155 regulates the proliferation and cell cycle of colorectal carcinoma cells by targeting E2F2. *Biotechnol Lett* 2014; **36**: 1743–1752.
36. Gracias DT, Stelekati E, Hope JL, Boesteanu AC, Doering TA, Norton J *et al.* The microRNA miR-155 controls CD8(+) T cell responses by regulating interferon signaling. *Nat Immunol* 2013; **14**: 593–602.
37. Xie Q, Chen X, Lu F, Zhang T, Hao M, Wang Y *et al.* Aberrant expression of microRNA 155 may accelerate cell proliferation by targeting sex-determining region Y box 6 in hepatocellular carcinoma. *Cancer* 2012; **118**: 2431–2442.
38. Liu S, Yin F, Zhang J, Wicha MS, Chang AE, Fan W *et al.* Regulatory roles of miRNA in the human neural stem cell transformation to glioma stem cells. *J Cell Biochem* 2014; **115**: 1368–1380.
39. Nicklas S, Okawa S, Hillje AL, González-Cano L, Del Sol A, Schwamborn JC *et al.* The RNA helicase DDX6 regulates cell-fate specification in neural stem cells via miRNAs. *Nucleic Acids Res* 2015; **43**: 2638–2654.
40. Yao H, Duan M, Yang L, Buch S. Platelet-derived growth factor-BB restores human immunodeficiency virus Tat-cocaine-mediated impairment of neurogenesis: role of TRPC1 channels. *J Neurosci* 2012; **32**: 9835–9847.
41. Yao H, Peng F, Dhillon N, Callen S, Bokhari S, Stehno-Bittel L *et al.* Involvement of TRPC channels in CCL2-mediated neuroprotection against tat toxicity. *J Neurosci* 2009; **29**: 1657–1669.
42. Hofman FM, Chen P, Incardona F, Zidovetzki R, Hinton DR. HIV-1 tat protein induces the production of interleukin-8 by human brain-derived endothelial cells. *J Neuroimmunol* 1999; **94**: 28–39.
43. Koller H, Schaal H, Freund M, Garrido SR, von Giesen HJ, Ott M *et al.* HIV-1 protein Tat reduces the glutamate-induced intracellular Ca2+ increase in cultured cortical astrocytes. *Eur J Neurosci* 2001; **14**: 1793–1799.
44. Malik S, Khalique H, Buch S, Seth P. A growth factor attenuates HIV-1 Tat and morphine induced damage to human neurons: implication in HIV/AIDS-drug abuse cases. *PLoS One* 2011; **6**: e18116.

Supplementary Information accompanies this paper on Cell Death and Differentiation website (http://www.nature.com/cdd)